Practical Approach to Programmable Analog Circuits With Memristors

Yuriy V. Pershin and Massimiliano Di Ventra

***Abstract*—We suggest an approach to use memristors (resistors with memory) in programmable analog circuits. Our idea consists in a circuit design in which low voltages are applied to memristors during their operation as analog circuit elements and high voltages are used to program the memristor's states. This way, as it was demonstrated in recent experiments, the state of memristors does not essentially change during analog mode operation. As an example of our approach, we have built several programmable analog circuits demonstrating memristor-based programming of threshold, gain and frequency. In these circuits the role of memristor is played by a memristor emulator developed by us.**

***Index Terms*—Analog circuits, analog memories, memory, resistance.**

I. Introduction

THE recent experimental demonstration of resistivity switching in TiO_2 thin films [1] and the establishment of a link between this result and more than 30-year-old theoretical description of memristors [2] (resistors with memory) have attracted a lot of attention to this exciting field. Memristive behavior is found in many different systems [1]–[20]. To interpret the experimental observations and predict a circuit behavior, a number of theoretical models were developed [1]–[3], [21]–[29], including SPICE models [27]–[29]. Memristors offer a nonvolatile memory storage within a simple device structure attractive for potential applications in electronics including the field of neuromorphic circuits as well, namely circuits which mimic the function and operation of neural cell networks in biological systems [30], [31]. Until now, most of the potential applications that have been proposed for these systems have relied on a binary mode of operation (on and off states of a memristor) while the understanding that memristors can be used as truly analog memory elements is only emerging [21], [30], [32].

A weaker interest in analog applications of memristors can be partially justified by the perception that TiO_2 thin films behave as ideal memristors. According to Chua's definition [2], the internal state of an ideal memristor depends on the integral of the voltage or current over time. Therefore, the use of ideal memristors as analog elements in, e.g., programmable analog circuits seems to be limited since their internal state, once programmed, would change significantly due to a dc component in current or applied voltage. Only *perfect* ac signals would not significantly change the memristor state so that the use of such devices seems to appear narrow. However, experimentally realizable memristors [10] are *not* ideal. In fact, these devices belong to the much more general class of memristive systems [3] (see the definition below) allowing for a more complex behavior, which is at the basis of our proposal.

At this point, a note should be made about the commonly used terminology and the terminology used in this paper. It appears that in the recent literature the term memristor has been used for both *ideal* memristors [2] and memristive devices and systems [3]. Indeed, we expect all experimental realizations of such devices to be not ideal. Therefore, there is no reason for two different names. This convention is used in the present paper, so that the term memristor will refer to *all* memristive systems and "ideal memristor" will be understood only in the sense of the definition in [2].

In the present paper, we suggest an approach to use resistors with memory in analog circuits based on threshold-type behavior of experimentally studied solid state memristors [9], [10]. Our main idea is to use low voltages in the analog mode of operation and high voltage pulses in order to program the memristor's state. In this way, we obtain a circuit element whose mode of operation is close to that of a digital potentiometer but its realization is much more simple. Our scheme represents an important application of a new class of emerging systems collectively called memory-circuit elements (*memelements*) [22]. Therefore, it may be of interest to scientists from such diverse disciplines as electrical engineering (in particular, from the area of tunable resistance research [33], [34]), physics, materials science, and even neuroscience.

This paper is organized as follows. Our approach to use memristors in programmable analog circuits is introduced in Section II. In Section III, we present a memristor emulator—an electronic circuit whose response is similar to that of a memristor. We will use this circuit in Section IV to demonstrate several applications of memristors in analog circuits including programmable threshold comparator, programmable gain amplifier, programmable switching thresholds Schmitt trigger, and programmable frequency relaxation oscillator. Concluding remarks are given in Section V.

II. Definitions and Main Concept

A. Circuit Elements With Memory

Before describing our approach, let us give formal definitions of memristors and briefly discuss their properties. To this end, we start from the general definition of circuit elements with

Manuscript received August 30, 2009; revised October 27, 2009; accepted November 22, 2009. Date of publication February 02, 2010; date of current version August 11, 2010. This work has been supported in part by the National Science Foundation under Grant DMR-0802830. This paper was recommended by Associate Editor M. Delgado-Restituto.

Yu. V. Pershin is with the Department of Physics and Astronomy and USC Nanocenter, University of South Carolina, Columbia, SC 29208 USA (e-mail: pershin@physics.sc.edu).

M. Di Ventra is with the Department of Physics, University of California, San Diego, La Jolla, CA 92093-0319 USA (e-mail: diventra@physics.ucsd.edu).

Digital Object Identifier 10.1109/TCSI.2009.2038539

memory which include also memcapacitors and meminductors [22]. Let us then introduce a set of n state variables x that describe the internal state of the system. Let us call $u(t)$ and $y(t)$ any two input and output variables [22], [35] that denote input and output of the system, such as the current, charge, voltage, or flux. With g we indicate a generalized response function. We then define a general class of nth-order u-controlled memory devices as those described by the relations [22]

$$y(t) = g(x, u, t)u(t) \tag{1}$$
$$\dot{x} = f(x, u, t) \tag{2}$$

where f is a continuous n-dimensional vector function, and we assume on physical grounds that, given an initial state $u(t = t_0)$ at time t_0, (2) admits a unique solution.

Memcapacitive and meminductive systems are special cases of (1) and (2), where the two constitutive variables that define them are charge and voltage for the memcapacitance, and current and flux for the meminductance. The properties of these systems can be found in [22]. In this paper, we will instead be concerned with a third class of memory devices—memristive systems. Using (1) and (2), we can define an nth-order voltage-controlled memristive system as that satisfying

$$I(t) = R_M^{-1}(x, V_M, t)V_M(t) \tag{3}$$
$$\dot{x} = f(x, V_M, t) \tag{4}$$

where x is a vector representing n internal state variables, $V_M(t)$ and $I(t)$ denote the voltage and current across the device. The quantity R_M is a scalar, called the memristance (for memory resistance) and its inverse R_M^{-1} is called memductance (for memory conductance).

Similarly, an nth-order current-controlled memristive system is described by

$$V_M(t) = R(x, I, t)I(t) \tag{5}$$
$$\dot{x} = f(x, I, t) \tag{6}$$

A charge-controlled memristor is a particular case of (5) and (6), when R depends only on the charge, namely

$$V_M(t) = R(q(t))I(t) \tag{7}$$

with the charge related to the current via time derivative $I = dq/dt$.

Several noteworthy properties can be identified for memristors [3]. For instance, these devices are passive provided $R_M^{-1}(x, V_M, t) > 0$ in (3), and do not store energy. Driven by a periodic current input, they also exhibit a "pinched hysteretic loop" in their current–voltage characteristics. Moreover, a memristor behaves as a linear resistor in the limit of infinite frequency and as a nonlinear resistor in the limit of zero frequency, assuming (4) admits a steady-state solution. The reason for this behavior is due to the system's ability to adjust to a slow change in bias (for low frequencies) and the reverse: its inability to respond to extremely high-frequency oscillations. We will explicitly demonstrate these properties with our memristor emulator presented in Section III.

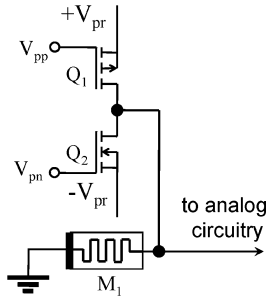

Fig. 1. Memristor-based digital potentiometer consisting of the memristor M_1 and a couple of FETs Q_1 and Q_2. The external control signals V_{pp} and V_{pn} are used to set (program) the resistance of memristor R_M between two limiting values R_1 and R_2. Here, V_{pr} is the memristor's programming voltage that should exceed the threshold voltage of memristor.

B. Memristors in Programmable Analog Circuits

Our main idea of using memristors in analog circuits is based on the following observation of the experimental results: the rate of memristance change depends essentially on the magnitude of applied voltage [9], [10]. At voltages below a certain threshold, the change of memristance is extremely slow, whereas at voltages above the threshold, V_T, it is fast. Therefore, we suggest to use memristors in analog circuits in such a way that in the analog mode of operation (when the memristor performs a useful function as an analog circuit element) only voltages of small magnitude (below the threshold) are applied to the device, while higher-amplitude voltages (above the threshold) are used only for programming. The programming voltages can be applied in the form of pulses. Each pulse changes the resistance of memristor by a discrete amount.

In this way, programmable memristors operate basically as digital potentiometers. However, there are several potential advantages of memristor-based digital potentiometers over the traditional ones. In particular, the size of a memristor can be very small, down to 30×30 nm^2 [31], allowing for higher density chips/smaller electronic components. The operation of memristor-based digital potentiometers requires less transistors since the information about resistance is written directly into a memristive medium. Finally, the resistance is remembered in the analog form potentially allowing for higher resolution. Recent examples of integration of TiO_2 memristors with conventional silicon electronics [36] and of a silicon-based memristive systems [11] have demonstrated the practical feasibility of integrated memristor-based electronic components.

Fig. 1 shows a simple memristor-based digital potentiometer which can operate as part of an analog circuit as we demonstrate below. For the sake of simplicity, one of the memristor's terminals is connected to the ground while another terminal is connected to analog circuitry and a pair of field effect transistors (FETs) that are used to program the memristor state. We use two external control signals V_{pp} and V_{pn} to open/close the FETs when needed. When one of these FETs is open, the programming voltage $\pm V_{pr}$ exceeding the threshold voltage of memristor V_T is applied and memristor's resistance changes in the direction determined by the applied voltage sign.

For definiteness, let us assume that the application of positive voltage increases R_M and application of negative voltage decreases R_M. Then, the following protocol of programming

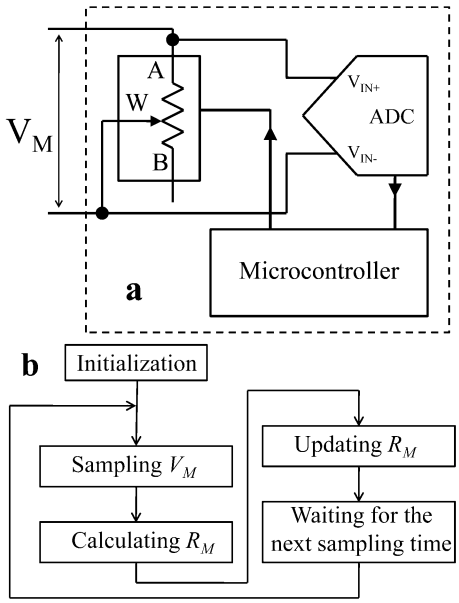

Fig. 2. (a) Memristor emulator consisting of the following units: a digital potentiometer, an analog-to-digital converter and a microcontroller. The A (or B) terminal and the Wiper of the digital potentiometer serve as the external connections of the memristor emulator. The resistance of the digital potentiometer is determined by a code written into it by the microcontroller. The code is calculated by the microcontroller according to (3) and (4). The analog-to-digital converter provides the value of voltage applied to the memristor emulator needed for the digital potentiometer code calculation. The applied voltage can be later converted to the current since the microcontroller knows the value of the digital potentiometer resistance and a current-controlled memristive system can be realized. In our implementation, we used a 256 positions 10 kΩ digital potentiometer AD5206 from Analog Device and microcontroller dsPIC30F2011 from Microchip with internal 12 bits ADC. (b) Block scheme of the memristor emulator's algorithm.

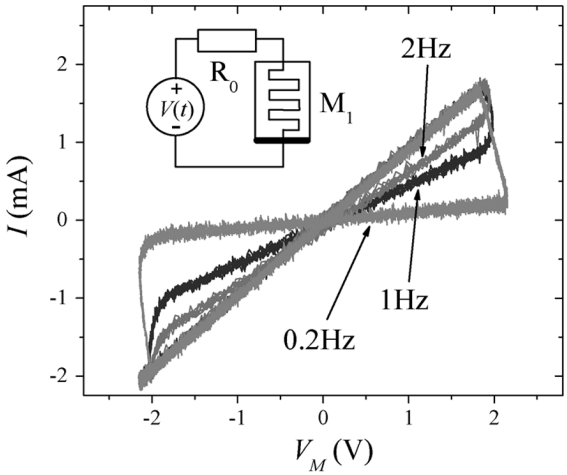

Fig. 3. I–V curves obtained with a memristor emulator wired as shown in the inset. The model given by (8) was used with $\alpha = 0, \beta = 62$ kΩ/V·s, $V_T = 1.75$ V, $R_{\min} = 1$ kΩ and $R_{\max} = 10$ kΩ. We used $V(t) = V_0 \sin(2\pi ft)$ as the applied voltage with $V_0 = 2.3$ V and f's as indicated on the plot. The curves are noisy because of the small value of $R_0 = 100$ Ω used to find the current and of limited resolution of our data acquisition system. We found that for the cases shown in this plot the initial value of R_M (in the present case equal to 1 kΩ) does not affect the long-time limit of the I–V curves.

can be employed. Since, at $t = 0$ we start with a possibly unknown value of R_M, the latter can be driven into the $R_{\max}$ state (state of maximum resistance) by connection of memristor M_1 to $+V_{pr}$ (using the "on" state of Q_1) for sufficiently long time (this time should be selected longer, or at least equal to the time required to switch R_M from $R_{\min}$—state of minimum resistance—to $R_{\max}$). After that, a connection of M_1 to $-V_{pr}$ (provided by the "on" state of Q_2) for a specific amount of time will switch R_M into a desired state. These manipulations can also be performed by application of a certain number of positive and negative fixed-width pulses. In fact, we have recently used pulse control of memristors in memristive neural networks [30].

The physical properties of TiO_2 memristors were reported and discussed in several papers [1], [10], [23]. The first theoretical model of TiO_2 memristors was suggested already in [1]. This model does not include any kind of threshold-type behavior and simply assumes that the resistance is proportional to the charge flown through device. However, subsequent work [10] has clearly shown that the charge-based model fails to describe the experimental results. In particular, Fig. 3(b) of [10] shows that a switching of memristor state occurs at high voltages while at low voltages sweep-down and sweep-up curves coincide. A first activation-type model explaining this feature was proposed by us [21] and has appeared in October 2008 in the cond-mat arxive [37]. A later publication [23] (in early 2009) explains the activation-type behavior of TiO_2 memristors by a nonlinear dopant drift in which, at low voltages, the change in memristor state is exponentially suppressed. These types of memristor behavior are precisely those needed for our proposal of analog programming.

III. Memristor Emulator

As of today, memristors are not yet available on the market. Therefore, in order to study memristor-based programmable circuits, we have built a memristor emulator [30]. The latter is a simple electronic scheme [see Fig. 2(a)] which can simulate a wide range of memristive systems. In particular, we have recently used it to simulate the behavior of synapses in simple neural networks [30]. The main element of the memristor emulator is a digital potentiometer whose resistance is continuously updated by a microcontroller and determined by pre-programmed equations of current-controlled or voltage-controlled memristive systems. A general form of equations describing a voltage-controlled memristive system is given by (3) and (4). These equations involve a voltage drop on the memristor V_M measured by the analog-to-digital converter (ADC). A block scheme of the memristor emulator operation algorithm is shown in Fig. 2(b). The algorithm's steps are self-explanatory.

In our experiments, we use an activation-type model of memristor [21], [30] inspired by recent experimental results [10]. Within our model, $R_M = x$ and (4) is written as (with the resistance acquiring the limiting values $R_{\min}$ and $R_{\max}$)

$$\dot{x} = (\beta V_M + 0.5(\alpha - \beta)[|V_M + V_T| - |V_M - V_T|]) \times \theta(x - R_{\min})\,\theta(R_{\max} - x) \quad (8)$$

where α and β are constants defining memristance rate of change below and above the threshold voltage V_T; V_M is the voltage on memristor and $\theta(\cdot)$ is the step function. To test that our emulator does indeed behave as a memristor, we have used the circuit shown in the inset of Fig. 3, in which an ac voltage is applied to the memristor emulator connected

TABLE I
COMPARISON TABLE OF A SOLID-STATE MEMRISTOR AND PRESENT VERSION OF MEMRISTOR EMULATOR

Parameter	Real memristor	Memristor emulator
Resistance range	Determined by the structure	$50\Omega < R < 10\text{k}\Omega$
Discretization of R	R changes continuously	256 steps
Frequency	Any	$\lesssim 50$Hz
Response	Determined by the structure	Determined by pre−programmed function
Applied V	Less than the breakdown voltage of the structure	0,+5V or -2.5,+2.5V
Supply V	Not needed	0,+5V or -2.5,+2.5V
Max. continuous I	Determined by the structure	$\pm$11mA

in series with a resistor which was used to determine the current. The obtained current-voltage (I-V) curves, presented in Fig. 3, demonstrate typical features of memristive systems such as pinched hysteresis loops and frequency-dependent hysteresis.

Table I shows a summary of main characteristics of a real memristor and of the present version of memristor emulator. In the case of memristor emulator, its characteristics are mainly limited by the electronic component that we use and can be significantly varied using different types of electronic components. As it is shown in the Table I, the resistance of the present memristor emulator can be tuned between 50 Ω (this low threshold is determined by unavoidable wiper resistance) and 10 kΩ in 256 steps, as determined by the digital potentiometer used. The ADC sampling frequency of 1 kHz limits the characteristic frequency of signals applied to memristor to approximately 50 Hz (20 points per period are reasonably enough to simulate a real memristor response). The voltage and current ratings of memristor emulator are determined by absolute maximum ratings of AD5206 digital potentiometer chip. By using a different hardware, the characteristics of memristor emulator can be improved. For example, the resolution can be easily increased to 1024 steps using a different digital potentiometer, and characteristic operational frequency can be as high as several tens of megahertz (MHz) using, e.g., a modern 2 Giga-sample ultra-high-speed ADC (such as, for example, ADC10D1000 offered by National Semiconductor). However, for the purpose of demonstration, high resolution and high frequencies are not required. This allows us to use inexpensive electronic components.

Moreover, in order to have a good correspondence between the response of a real memristor and that of a memristor emulator, it is extremely important to have an appropriate device model. This model, in terms of equations, is pre-programmed into the microcontroller and the behavior of the memristor emulator would follow closely the given model (within the limits listed in Table I). The model we employ [given by (8)] is quite simple. However, it contains all important physics of solid-state memristive devices whose behavior derives from activation-type processes.

IV. APPLICATIONS

There is certainly a number of analog circuits where a memristor can operate under the conditions described in Section II. Here, we show few examples of those applications.

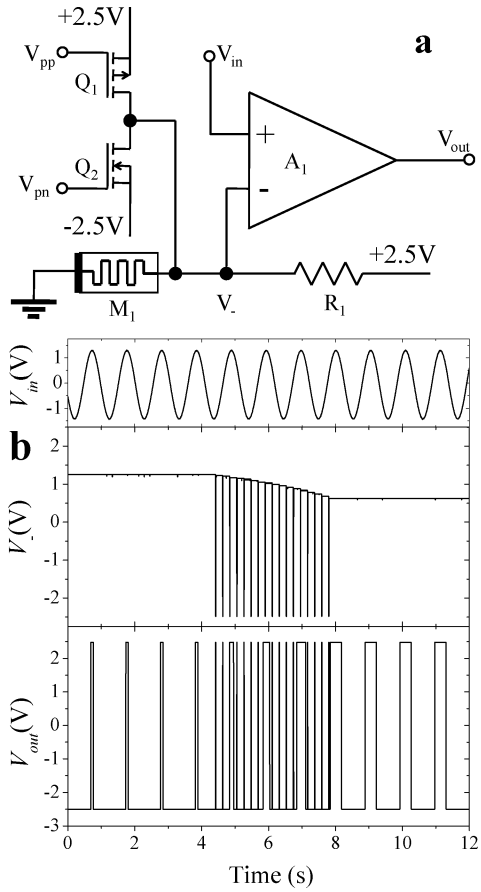

Fig. 4. (a) Schematics of a programmable threshold comparator. Here, M_1 is the memristor, $R_1 = 10$ kΩ and A_1 is an operational amplifier. In our experiments, we used operational amplifier model TLV2770 (Texas Instruments) that was powered by a dual polarity ± 2.5 V power supply. (b) Programmable threshold comparator response to the input voltage $V_{\text{in}} = V_0 \sin(2\pi f t)$ with $V_0 = 1.3$ V and $f = 1$ Hz, and several negative programming pulses of 10 ms width applied in the time interval between 4 and 8 seconds. V_{in} is the input voltage applied to the positive input of the operational amplifier, V_- is the voltage on the negative input of the operational amplifier, and V_{out} is the signal at the output of the operational amplifier. Each 10 ms voltage pulse changes R_M by approximately 430 Ω causing a gradual decrease of the comparator threshold.

A. Programmable Threshold Comparator

Let us start by demonstrating memristor-based programmable analog circuit operations with arguably the simplest case—a programmable threshold comparator as shown in Fig. 4(a). The design of this circuit, as well as of all other circuits discussed below, involves the memristor-based digital potentiometer block shown in Fig. 1. In the analog mode of operation, both FETs are off. In all our practical examples we build a scheme in such a way that the maximum voltage drop on memristor is always smaller than the threshold voltage of memristor which was selected to be equal to 1.75 V. When possible, it is desirable to apply to memristor as low voltages as possible in order to further reduce the slow change of memristor state below its threshold.

In the programmable threshold comparator circuit, the comparator threshold is determined by the voltage on the memristor given by

$$V_- = V_{\text{cc}} R_M / (R_M + R_1) \tag{9}$$

where $V_{\rm cc} = 2.5$ V is the power supply voltage, and R_1 is the value of the resistance of the "standard" resistor. If the signal amplitude at the positive input $V_{\rm in}$ exceeds V_-, then output signal $V_{\rm out}$ is equal to the saturation voltage of the operational amplifier (which in the present case is close to $+2.5$ V). In the opposite case, $V_{\rm out}$ is close to -2.5 V.

Fig. 4(b) shows the operation of the programmable threshold comparator scheme when a sinusoidal voltage with an amplitude of 1.3 V is applied to its input. At the initial moment of time, the resistance of memristor is set to $R_M = 10$ kΩ. That means that $V_- = 1.25$ V and $V_{\rm in}$ exceeds V_- only for a short period of time. As a result, we observe a set of narrow positive pulses at the output $V_{\rm out}$. The application of a train of negative pulses in the time interval between 4 and 8 seconds re-programs the memristor state by lowering the comparator threshold. This can be observed in a smaller V_- and wider output pulses starting at $t = 8$ s.

B. Programmable Gain Amplifier

The next circuit we consider is a programmable gain amplifier whose general scheme is shown in Fig. 5(a). As in the usual non-inverting amplifier configuration, the input signal $V_{\rm in}$ is applied to the positive input of the operational amplifier $\rm A_1$, while one of the two resistors, connected to the negative input is substituted by a memristor $\rm M_1$. The gain of such amplifier (R_1 is the value of the resistance of the "standard" resistor)

$$V_{\rm out}/V_{\rm in} = 1 + R_1/R_M \tag{10}$$

is determined by the value of memristance R_M which can be selected (programmed) between two limiting values $R_{\rm min}$ and $R_{\rm max}$ using two field-effect transistors (FETs). The desirable regime of operation that minimizes the voltage applied to the memristor is $R_M \ll R_1$.

Fig. 5(b) and 5(c) demonstrates operation of the programmable gain amplifier shown in Fig. 5(a). The amplifier's gain is controlled using pulses of constant width. The pulse width is 10 ms in Fig. 5(b) and 20 ms in Fig. 5(c). In both cases, at the initial moment of time $t = 0$, the memristor is in its highest resistance state $R_M = R_{\rm max} = 10\ k\Omega$ and, according to (10), the circuit gain is about 2. Correspondingly, the input signal $V_{\rm in} = 0.2$ V results in $V_{\rm out} = 0.4$ V at that time, as it can be seen in Fig. 5(b) and 5(c).

Application of pulses at V_- changes the value of R_M and, correspondingly, the gain. Each negative pulse at V_- decreases the value of R_M while each positive pulse increases R_M. Steps in the output signal $V_{\rm out}$ (separated by spikes due to the voltage pulses during programming) correspond to different values of circuit's gain (the input voltage $V_{\rm in}$ is kept constant during the experiment). For the selected memristor parameters, the circuit gain changes approximately from 2 to 11. We demonstrate in Fig. 5(c) that longer pulses produce larger changes in R_M allowing for coarser control of the gain.

C. Programmable Switching Thresholds Schmitt Trigger

Fig. 6(a) shows schematics of a programmable switching thresholds Schmitt trigger in the inverted configuration. This circuit behaves as an inverted comparator with the switching

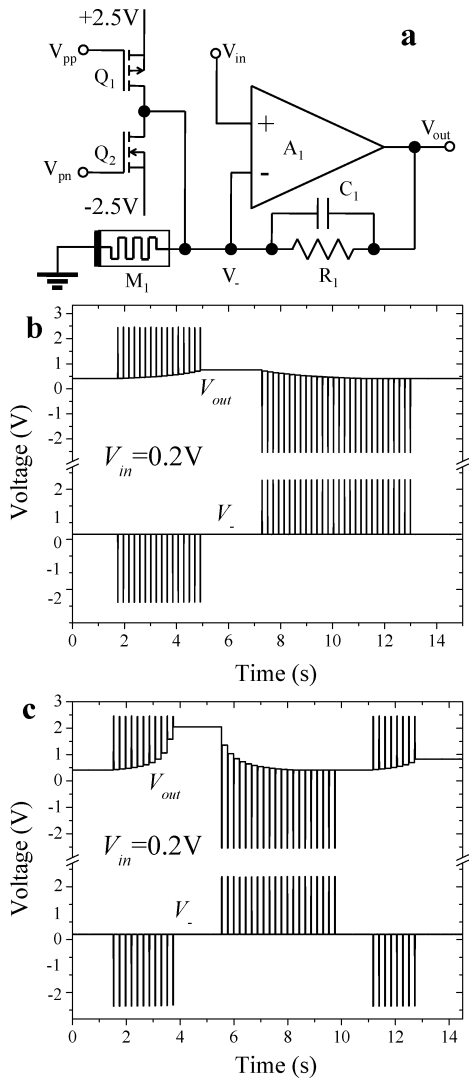

Fig. 5. (a) Schematics of a programmable gain amplifier with memristor. The operational amplifier $\rm A_1$ is connected in the standard non-inverting amplifier configuration with a memristor $\rm M_1$ replacing a resistor. Two FETs ($\rm Q_1$ and $\rm Q_2$) are used to program the resistance of the memristor thus selecting the amplifier gain. The capacitor $\rm C_1 = 0.1\ \mu F$ is used for noise suppression. (b) Programming of gain using 10-ms width pulses. In these measurements, the input voltage $V_{\rm in} = 0.2$ V is permanently supplied while positive and negative pulses change the state of memristor and correspondingly circuit's gain. As a result, we observe a set of steps in the output signal. (c) Coarser control of gain using 20 ms width pulses.

thresholds given by $\pm(R_M/R_1)V_{\rm sat}$ where, for our circuit, $V_{\rm sat} = 2.5$ V. When we apply programming pulses to M_1, its resistance R_M changes as well as the switching thresholds of Schmitt trigger. This type of behavior is clearly seen in Fig. 6(b). Here, at the initial moment of time, the memristor is in a low resistance state and, correspondingly, the switching thresholds are low. Therefore, the switchings (changes of $V_{\rm out}$ from -2.5 V to 2.5 V and vice-versa) occur close to the moment of time when $V_{\rm in}$ is close to zero as it follows from the positions of the intersection points of $V_{\rm in}$ with $V_{\rm out}$ curves in the upper panel of Fig. 6(b).

A train of positive pulses applied to the memristor [see V_+ curve in Fig. 6(b)] in a time interval between 2 and 4 s increases R_M and, consequently, the Schmitt trigger's switching threshold. As a result, the upper panel in Fig. 6(b) demonstrates

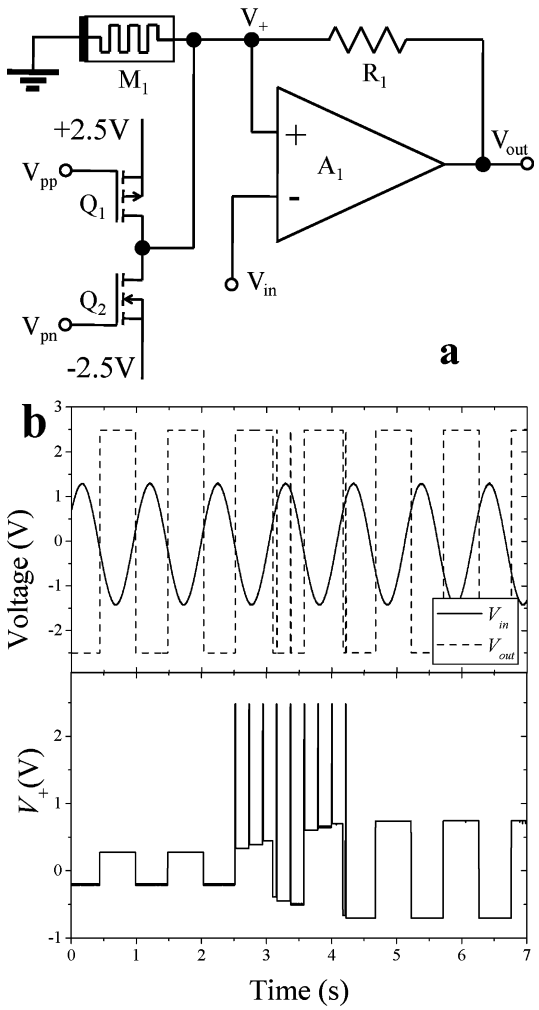

Fig. 6. (a) Schematics of a programmable switching thresholds Schmitt trigger with memristor. Here, $R_1 = 10$ kΩ. (b) Programmable switching thresholds Schmitt trigger response to the input voltage $V_{\rm in} = V_0 \sin(2\pi f t)$ with $V_0 = 1.3$ V and $f = 1$ Hz, and several positive programming pulses of 10 ms width applied in the time interval between 2 and 4 s.

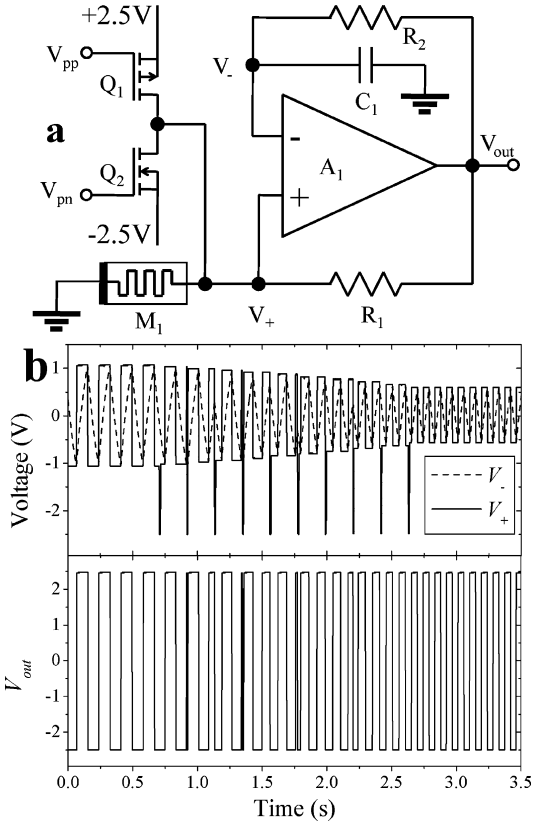

Fig. 7. (a) Schematics of a programmable frequency relaxation oscillator with memristor. Here, $R_1 = R_2 = 10$ kΩ and $C = 10\,\mu$F. (b) Oscillating signals in the different points of the programmable frequency relaxation oscillator. The lower panel demonstrates an increase in the oscillation frequency as R_M is decreased by several negative pulses applied to V_+.

that switching of $V_{\rm out}$ occurs at different values of $V_{\rm in}$ when $t > 4$ s.

D. Programmable Frequency Relaxation Oscillator

As a final example we consider a programmable frequency relaxation oscillator. This is schematically shown in Fig. 7(a). The relaxation oscillator is a well-known circuit which automatically oscillates because of the negative feedback added to a Schmitt trigger by an RC circuit. The period of oscillations is determined by both the RC components and switching thresholds of the Schmitt trigger. Therefore, in order to control the relaxation oscillator frequency, we use a memristor-based digital potentiometer to vary switching thresholds of the Schmitt trigger, similarly to what is shown in Fig. 6(a).

Fig. 7(b) demonstrates that a decrease of the memristor resistance R_M results in an increase of the relaxation oscillator frequency. As it is demonstrated in the upper panel of Fig. 7(b), the decrease of the switching threshold results in a faster capacitor charging time (because now the capacitor has to charge to a smaller voltage). Via this mechanism, the memristor-based digital potentiometer then determines the frequency of oscillations.

V. Discussion and Conclusion

Having demonstrated the operation of memristor-based programmable analog circuits, we would like to discuss certain practical aspects of using the suggested approach with solid-state memristors that are presently investigated. First of all, it should be mentioned that although the rate of memristance change at low voltages is very small as observed in certain experiments [10], it can eventually lead to a drift (increase or decrease depending on particular application scheme) of R_M at long times. Currently, it is difficult to estimate this effect, in part because of the lack of experimental data. However, this parasitic effect becomes less important at low voltages applied to the memristor and, in practice, can be corrected by periodic re-setting of R_M or/and circuit calibration. We also can not exclude the possibility that the drift would become important only after several months or years of device operation.

Another important point is the precision of the memristor state programming. To program a desired value of memristance with a given precision we should either have enough information on the memristor operation model, parameters (and have reproducibly operating memristors), or provide pulses of precise amplitude and duration. Alternatively we need to implement, electronically, a suitable calibration procedure allowing for correction of non-precise programming. Technical solutions

for the tasks mentioned above can certainly be found. Concerning reproducibility of memristive behavior, experiments with TiO_2 thin films demonstrate a significant amount of noise in hysteresis curves [10]. Possibly, the resistance change effect in colossal magnetoresistive thin films [9] is more suitable for analog-mode memristor applications.

In conclusion, we have suggested an approach for a practical application of memristors in programmable analog circuits. To demonstrate experimentally our approach, we have built several memristor-based programmable analog circuits using a memristor emulator. The latter is a scheme that uses inexpensive off-the-shelf components and can, therefore, be built quite easily in any electronic lab. By applying a train of pulses, we have achieved programming of different properties such as threshold, gain and frequency. We have thus shown that a memristor with a control scheme provides a simple realization of digital potentiometers and, therefore, can find useful and broad-range applications in electronics.

ACKNOWLEDGMENT

The authors are indebted to B. Mouttet for pointing out [9] to them.

REFERENCES

[1] D. B. Strukov, G. S. Snider, D. R. Stewart, and R. S. Williams, "The missing memristor found," *Nature*, vol. 453, no. 7191, pp. 80–83, 2008.

[2] L. O. Chua, "Memristor—The missing circuit element," *IEEE Trans. Circuit Theory*, vol. 18, no. 5, pp. 507–519, 1971.

[3] L. O. Chua and S. M. Kang, "Memristive devices and systems," *Proc. IEEE*, vol. 64, no. 2, pp. 209–223, 1976.

[4] Y. V. Pershin and M. Di Ventra, "Spin memristive systems: Spin memory effects in semiconductor spintronics," *Phys. Rev. B*, vol. 78, no. 11, pp. 113309/1–113309/4, 2008.

[5] T. Driscoll, H. T. Kim, B. G. Chae, M. Di Ventra, and D. N. Basov, "Phase-transition driven memristive system," *Appl. Phys. Lett.*, vol. 95, no. 4, pp. 043503/1–043503/3, 2009.

[6] T. Driscoll, H.-T. Kim, B.-G. Chae, B.-J. Kim, Y.-W. Lee, N. M. Jokerst, S. Palit, D. R. Smith, M. Di Ventra, and D. N. Basov, "Memory metamaterials," *Science*, vol. 325, no. 5947, pp. 1518–1521, Sept. 18, 2009.

[7] Y. V. Pershin and M. Di Ventra, "Frequency doubling and memory effects in the spin Hall effect," *Phys. Rev. B*, vol. 79, no. 15, pp. 153307/1–153307/4, 2009.

[8] X. Wang, Y. Chen, H. Xi, H. Li, and D. Dimitrov, "Spintronic memristor through spin-torque-induced magnetization motion," *IEEE Electron Device Lett.*, vol. 30, no. 3, pp. 294–297, 2009.

[9] S. Liu, N. Wu, and A. Ignatiev, "Electric-pulse-induced reversible resistance change effect in magnetoresistive films," *Appl. Phys. Lett.*, vol. 76, no. 19, pp. 2749–2751, 2000.

[10] J. J. Yang, M. D. Pickett, X. Li, D. A. A. Ohlberg, D. R. Stewart, and R. S. Williams, "Memristive switching mechanism for metal/oxide/metal nanodevices," *Nat. Nanotechnol.*, vol. 3, no. 7, pp. 429–433, 2008.

[11] S. H. Jo, K.-H. Kim, and W. Lu, "High-density crossbar arrays based on a si memristive system," *Nano Lett.*, vol. 9, no. 2, pp. 870–874, 2009.

[12] D. Stewart, D. Ohlberg, P. Beck, Y. Chen, R. Williams, J. Jeppesen, K. Nielsen, and J. Stoddart, "Molecule-independent electrical switching in pt/organic monolayer/ti devices," *Nano Lett.*, vol. 4, no. 1, pp. 133–136, 2004.

[13] V. V. Erokhin, T. S. Berzina, and M. P. Fontana, "Polymeric elements for adaptive networks," *Crystallogr. Rep.*, vol. 52, no. 1, pp. 159–166, 2007.

[14] H. Choi, H. Jung, J. Lee, J. Yoon, J. Park, D.-J. Seong, W. Lee, M. Hasan, G.-Y. Jung, and H. Hwang, "An electrically modifiable synapse array of resistive switching memory," *Nanotechnology*, vol. 20, no. 34, pp. 345201/1–345201/5, 2009.

[15] N. Gergel-Hackett, B. Hamadani, B. Dunlap, J. Suehle, C. Richter, C. Hacker, and D. Gundlach, "A flexible solution-processed memristor," *IEEE Electron Device Lett.*, vol. 30, no. 7, pp. 706–708, Jul. 2009.

[16] X. Chen, G. Wu, P. Jiang, W. Liu, and D. Bao, "Colossal resistance switching effect in pt/spinel-mgzno/pt devices for nonvolatile memory applications," *Appl. Phys. Lett.*, vol. 94, no. 3, pp. 033501/1–033501/3, 2009.

[17] K. Oka, T. Yanagida, K. Nagashima, H. Tanaka, and T. Kawai, "Nonvolatile bipolar resistive memory switching in single crystalline NiO heterostructured nanowires," *J. Amer. Chem. Soc.*, vol. 131, no. 10, pp. 3434–3435, 2009.

[18] L. Chen, Z. Liu, Y. Xia, K. Yin, L. Gao, and J. Yin, "Electrical field induced precipitation reaction and percolation in Ag30Ge17Se53 amorphous electrolyte films," *Appl. Phys. Lett.*, vol. 94, no. 16, pp. 162112/1–162112/3, 2009.

[19] B. Standley, W. Bao, H. Zhang, J. Bruck, C. N. Lau, and M. Bockrath, "Graphene-based atomic-scale switches," *Nano Lett.*, vol. 8, no. 10, pp. 3345–3349, 2008.

[20] G. S. Rose and M. R. Stan Jr., "A programmable majority logic array using molecular scale electronics," *IEEE Trans. Circuits Syst. I, Reg. Papers*, vol. 54, no. 11, pp. 2380–2390, Nov. 2007.

[21] Y. V. Pershin, S. La Fontaine, and M. Di Ventra, "Memristive model of amoeba's learning," *Phys. Rev. E*, vol. 80, p. 021926, 2009.

[22] M. Di Ventra, Y. V. Pershin, and L. O. Chua, "Circuit elements with memory: Memristors, memcapacitors and meminductors," *Proc. IEEE*, vol. 97, pp. 1717–1724, 2009.

[23] D. B. Strukov and R. S. Williams, "Exponential ionic drift: Fast switching and low volatility of thin-film memristors," *Appl. Phys. A-Mater. Sci. Process.*, vol. 94, no. 3, pp. 515–519, 2009.

[24] D. B. Strukov, J. L. Borghetti, and R. S. Williams, "Coupled ionic and electronic transport model of thin-film semiconductor memristive behavior," *Small*, vol. 5, no. 9, pp. 1058–1063, 2009.

[25] C. Cagli, F. Nardi, and D. Ielmini, "Modeling of set/reset operations in NiO-based resistive-switching memory devices," *IEEE Trans. Electron Devices*, vol. 56, no. 8, pp. 1712–1720, Aug. 2009.

[26] Y. N. Joglekar and S. J. Wolf, "The elusive memristor: Properties of basic electrical circuits," *Eur. J. Phys.*, vol. 30, no. 4, pp. 661–675, 2009.

[27] S. Benderli and T. A. Wey, "On spice macromodelling of TiO2 memristors," *Electron. Lett.*, vol. 45, no. 7, pp. 377–378, 2009.

[28] Z. Biolek, D. Biolek, and V. Biolkova, "Spice model of memristor with nonlinear dopant drift," *Radioengineering*, vol. 18, no. 2, pt. 2, pp. 210–214, 2009.

[29] Z. Biolek, D. Biolek, and V. Biolkova, "Spice modeling of memristive, memcapacitative and meminductive systems," in *Proc. ECCTD'09, Eur. Conf. on Circuit Theory and Design*, Aug. 23–27, 2009, pp. 249–252.

[30] Y. V. Pershin and M. Di Ventra, "Experimental demonstration of associative memory with memristive neural networks," 2009 [Online]. Available: http://arXiv.org/abs/arXiv:0905.2935

[31] G. S. Snider, "Cortical computing with memristive nanodevices," *Sci-DAC Rev.*, vol. 10, pp. 58–65, 2008.

[32] A. Delgado, "Input—output linearization of memristive systems," in *Nanotechnol. Mater. Devices Conf.*, Traverse City, MI, June 2–5, 2009.

[33] E. Ozalevli and P. E. Hasler, "Tunable highly linear floating-gate CMOS resistor using common-mode linearization technique," *IEEE Trans. Circuits Syst. I, Reg. Papers*, vol. 55, no. 4, pp. 999–1010, May 2008.

[34] K. H. Wee and R. Sarpeshkar, "An electronically tunable linear or nonlinear MOS resistor," *IEEE Trans. Circuits Syst. I, Reg. Papers*, vol. 55, no. 9, pp. 2573–2583, Oct. 2008.

[35] L. Chua, "Nonlinear circuit foundations for nanodevices—Part I: The four-element torus," *Proc. IEEE*, vol. 91, no. 11, pp. 1830–1859, Nov. 2003.

[36] J. Borghetti, Z. Li, J. Straznicky, X. Li, D. A. A. Ohlberg, W. Wu, D. R. Stewart, and R. S. Williams, "A hybrid nanomemristor/transistor logic circuit capable of self-programming," *Proc. Nat.. Acad. Sci. U. S. A.*, vol. 106, no. 6, pp. 1699–1703, 2009.

[37] Y. V. Pershin, S. La Fontaine, and M. Di Ventra, "Memristive model of amoeba's learning," 2008 [Online]. Available: ArXiv:0810.4179

Yuriy V. Pershin received the Ph.D. degree in theoretical physics from the University of Konstanz, Germany, in 2002.

He is currently Assistant Professor of Physics at the University of South Carolina, Columbia. During his career, he has been with the University of California, San Diego, Michigan State University, Clarkson University, and Grenoble High Magnetic Field Laboratory. He has authored over 40 research papers, and 3 reviews. His recent research interests span broad areas of nanotechnology, including physics of semiconductor nanodevices, spintronics and biophysics.

Massimiliano Di Ventra received the Ph.D. degree from the Ecole Polytechnique Federale de Lausanne (CH) in 1997.

He is currently Professor of Physics at the University of California, San Diego. He is an expert is in the theory of electronic and transport properties of nanoscale systems, and has delivered more than 100 invited talks worldwide on these topics. He has co-edited the textbook *Introduction to Nanoscale Science and Technology* (Springer, 2004) for undergraduate students, and is the author of the graduate-level textbook *Electrical Transport in Nanoscale Systems* (Cambridge Univ. Press, 2008).

Dr. Di Ventra serves on the editorial board of several scientific journals and has won numerous awards and honors, including the NSF Early CAREER Award, the Ralph E. Powe Junior Faculty Enhancement Award, and fellowship in the Institute of Physics.